



## Nonlinear Structural Performance of Self-Centring Bridge Piers with Shape Memory Alloy Bars

**Sedef Kocakaplan** –Bursa Technical University, Bursa, Turkey, e-mail: ([sedef.kocakaplan@btu.edu.tr](mailto:sedef.kocakaplan@btu.edu.tr))

**Ehsan Ahmadi** – Birmingham City University, Birmingham, United Kingdom, e-mail: ([ehsan.ahmadi@bcu.ac.uk](mailto:ehsan.ahmadi@bcu.ac.uk))

**Mehdi Kashani** – University of Southampton, Southampton, United Kingdom, e-mail: ([mehdi.kashani@soton.ac.uk](mailto:mehdi.kashani@soton.ac.uk))

**Abstract:** Application of precast post-tensioned segmental (PPS) bridge piers has increased in recent years in accelerated bridge construction (ABC). In order to increase the use of PPS piers in high seismicity regions, this work investigates the nonlinear behaviour of a segmental bridge pier with unbonded post-tensioned superelastic Shape Memory Alloy (SMA) bars through a Finite Element (FE) framework. A parametric study is conducted on the key design parameters through a series of nonlinear cyclic analysis to investigate the energy dissipation capacity of the SMA-equipped piers. Furthermore, seismic performance of the piers is investigated using far-field ground motions and incremental dynamic analysis (IDA) is performed. It is found that length, area, and post-tensioning ratio of the SMA bars affect the energy dissipation capacity of the piers, and an optimal design of the bars is required to reach the highest energy dissipation possible. The IDA analysis showed that PPS piers with SMA bars reduced the top drift responses of the piers.

**Keywords:** Piers; bridge; shape memory alloy; self-centring

### 1. Introduction

In recent years, accelerated bridge construction (ABC) has led to substantial application of precast post-tensioned segmental (PPS) bridge piers. PPS bridge piers (Shim et al. (2008), Dawood et al. (2012)) have been introduced as a substitute to cast-in-place (CIP) bridge piers in accelerated bridge construction (Tazarv (2016), Haber (2013)). PPS piers can reduce the residual displacement through discrete hinges between the segments (i.e. joints). Furthermore, the self-centring mechanism is provided through the post-tensioning tendons running along the pier length leading to a more seismically resilient system. In order to increase the use of PPS piers in highly-seismic regions, low energy dissipation capacity of the piers should be addressed. Therefore, in this study, energy dissipation capacity of the PPS piers with unbonded post-tensioned superelastic shape memory alloy (SMA) bars investigated using a Finite Element (FE) method. The SMA bars are used at the edge of the segments to increase damping capability of the pier and improve self-centring capacity of the entire pier. It is well known that SMA bars can dissipate energy of the structure through their nonlinear deformations, and return to their initial state after loading events (Song et al. (2006), Saiidi and Wang (2006), DesRoches et al. (2004)). PPS piers are modelled using experimentally validated OpenSees (McKenna (2011)) numerical model (Ahmadi and Kashani (2019)). Parametric study is performed to understand how post-tensioning tendon and SMA bars affect the energy dissipation capacity of the pier through a series of nonlinear cyclic analysis. Furthermore, selected examples of the PPS piers are subjected to far-field ground motions, and results are compared to ones without SMA bars.

## 2. Finite Element Model of PPS Piers

In order to investigate the energy dissipation capacity of PPS piers with SMA bars, different number of segments are considered in this study. Figure 1a shows an exemplary PPS pier with SMA bars. The piers consist of four segments, and its total height is  $H=2000$  mm. The precast concrete segments have width,  $B=500$  mm and height,  $h=500$  mm. The other PPS piers studied in this work are composed of two, six and ten segments. The post-tensioning tendons are run along the pier length and provide self-centring mechanism. Bridge deck modelled at the top of the pier and represented as lumped mass (See Figure 1a.).

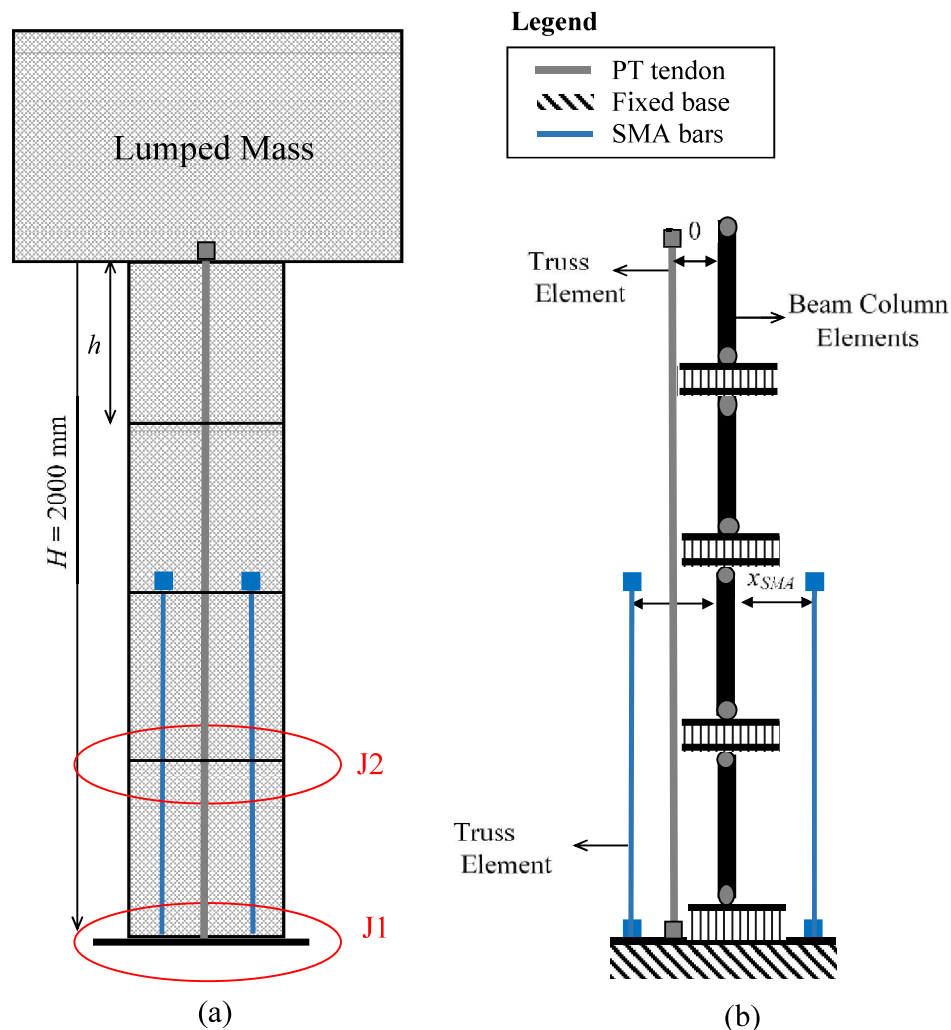


Fig. 1 – (a) The PPS pier, (b) section with SMA bars (section 1-1), (c) section with no SMA bars (section 2-2), and (d) OpenSees model.

To increase the energy dissipation capacity, unbounded superelastic SMA bars are used at the bottom the segments. Figure 1b represents the OpenSees model used for the PPS piers. The details of the OpenSees model can be found in Ahmadi and Kashani (2019). Each compression zone (see Figure 1b) is modelled as a set of axial zero-length spring elements.

An elastic zero-tension uniaxial material model is assigned to the joints, which can simulate the joint openings and compression forces at the contact surfaces. Inertial effects of the bridge deck are considered by applying lumped horizontal and vertical masses to the top node of the pier. These masses are equivalent to the axial force acting on the pier. SMA bars are modelled using Truss Elements, and the idealized constitutive model for the SMA material is used based on the experimental results valid in Li et al. (2017). The SMA material model including the post-tensioning stress was implemented by the authors in OpenSees.

### 3. Numerical Results and Discussion

In this section, in order to investigate the nonlinear cyclic performance of the PPS piers with SMA bars, a comprehensive parametric study is performed. The investigated key design parameters for the nonlinear cyclic analysis are: (i) number of segments or aspect ratio, (ii) length, area, and post-tensioning ratio of the SMA bars (bars-to-segment area ratio), and (iii) area and post-tensioning ratio of the tendon (tendon-to-segment area ratio). The key design parameters are decided according their possible effect on the energy dissipation capacity of the piers.

The capacity curves (i.e. base shear verses drift) are obtained for a full cyclic loop ( $\pm 6\%$  drift) to examine the nonlinear cyclic behaviour of the piers. The varied key design parameters are given in Table 1. Here,  $\alpha_t$  and  $\alpha_{sma}$  are the post-tensioning ratios of the tendon and SMA bars respectively;  $\rho_t$  is the tendon-to-segment area ratio, and  $\rho_{sma}$  is the SMA bars-to-segment ratio;  $n$  is the number of segments; and  $J_{sma}$  is the joint number at which the top node of the SMA bars is located. The bottom end of the all SMA bars are connected to the fixed base and the top end node location varies as shown by  $J_{sma}$  representing the length of the SMA bars (see Figure 1a).

Table 1. Design Parameters

Design Parameters	$n$	$N/(f_c A_c)$	$\alpha_t$	$\rho_t$	$J_{sma}$	$\alpha_{sma}$	$\rho_{sma}$
Values	2	0.2	0.0	0.010	2	0.0	0.005
	4	0.2	0.2	0.015	3	0.3	0.01
	6	0.2	0.4	0.020	4	0.6	0.015
	10	0.2	0.6	-	5	-	0.025

Figure 2 shows the effects of SMA bars' area ratio,  $\rho_{sma}$  on the cyclic behaviour of the piers for an exemplary pier with  $n=4$ , for different length of SMA bars,  $J_{sma}$ . For small area of SMA bars,  $\rho_{sma} = 0.005$ , the pier experiences a slight energy dissipation, while energy dissipation capacity of the pier becomes highest for  $\rho_{sma} = 0.025$  (see Figure 2b and 2c). For large  $\rho_{sma}$  and  $J_{sma}$  small the SMA bars become very stiff (due to no gap opening of the pier occurring in higher drifts) and the pier show no energy dissipation, which can be observed in Figure 2a for  $\rho_{sma}=0.025$  and  $J_{sma} = 2$ . Therefore, there is an optimal SMA bars' area and length at which the maximum energy dissipation capacity of the pier is reached.

Figure 3a illustrates the post-tensioning effect of the SMA bars on the energy dissipation capacity of the exemplary pier. According to figure, increase in the post-tensioning ratio of the SMA bars results in higher energy dissipation capacity for the pier. Figures 3b-3d show the stress-strain ratio of the right edge SMA bars with change in post-tensioning ratios. Both linear and nonlinear behaviour are observed in SMA bars with the displacement of

the piers. According to figures, increasing the post-tensioning ratio reduces the linear behaviour and increases the nonlinear behaviour, in which higher energy dissipation capacity is reached.

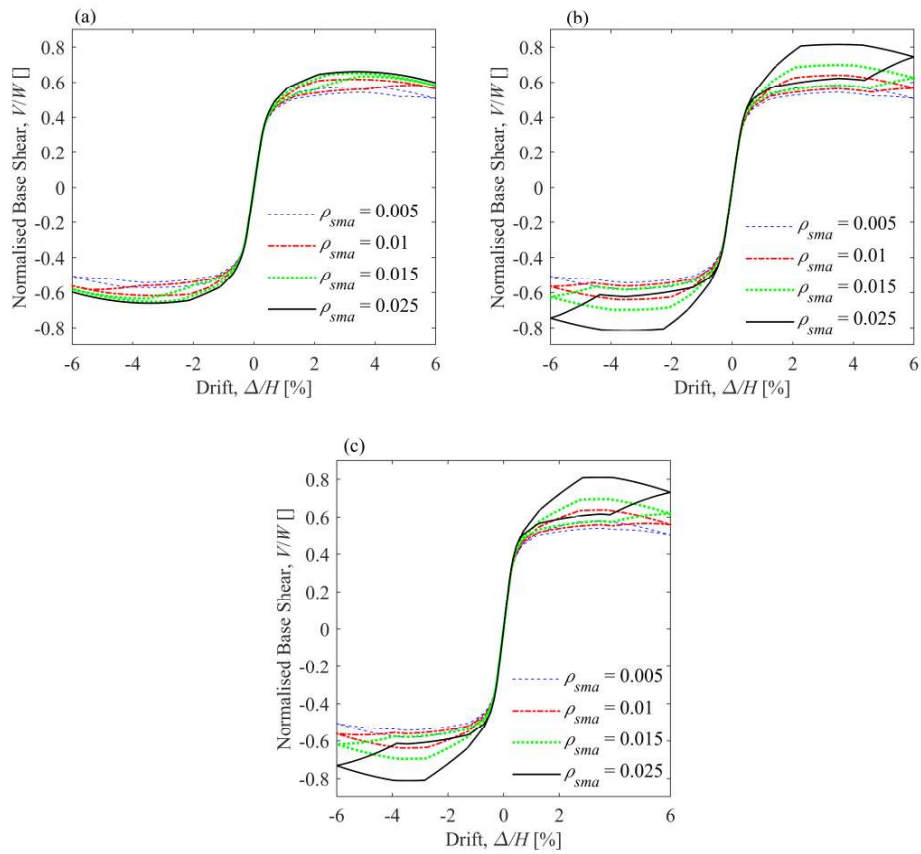


Fig. 2 – Effects of SMA bars' area for the pier with  $n=4$ ,  $\alpha_t = 0.6$ ,  $\rho_t = 0.015$ ,  $\alpha_{sma} = 0.3$ , (a)  $J_{sma} = 2$  (b)  $J_{sma} = 3$  (c)  $J_{sma} = 4$ .

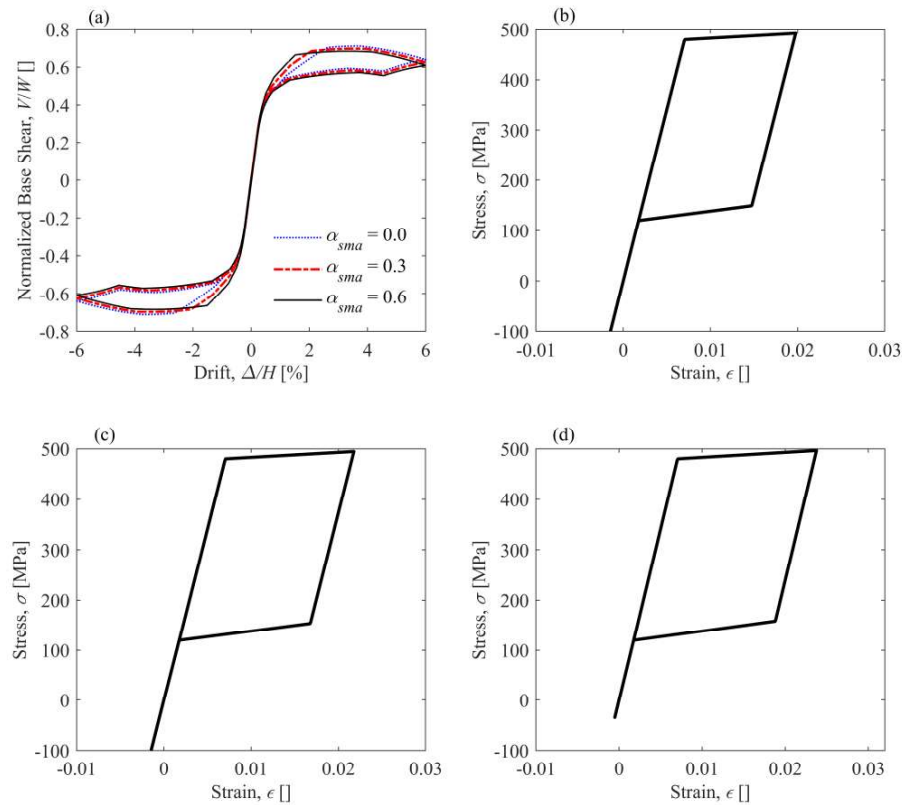


Fig. 3 – (a) Post-tensioning effect of the SMA bars on the energy dissipation capacity of the exemplary pier ( $n=4$ ,  $\alpha_t = 0.6$ ,  $\rho_t = 0.015$ ,  $\rho_{sma} = 0.015$ ,  $J_{sma} = 3$ ); the corresponding stress-strain behaviour of the SMA bars for: (b)  $\alpha_{sma} = 0$ , (c)  $\alpha_{sma} = 0.3$ , and (d)  $\alpha_{sma} = 0.6$ .

PPS pier with having one of the highest energy dissipation capacity is chosen in order to investigate the seismic performance of the piers. A constant-stiffness Rayleigh damping is used for the piers with damping ratio of 5% for all elements in the models. The properties of the pier are, the location of the top end of SMA is  $J=3$ ,  $\rho_t$  is equal to 0.02,  $\alpha_t$  is equal to 0.4,  $\alpha_{sma}$  is equal to 0.3, and  $\rho_{sma}$  is equal to 0.025. Moreover, results are also compared with the pier with no SMA bars. The piers are subjected to seven component pairs of horizontal far-field ground motions available in Pacific Earthquake Engineering Research Centre (PEER) Next-Generation Attenuation (NHA) database (NGA-West2,2017). Figure 4 and Figure 5 show IDA curves and median IDA curves for top drift and normalised base shear-time history of the PPS piers. According to results, Piers with SMA bars reduced the drift response approximately while resulted in increased normalised base shear due to having a stiffer system.

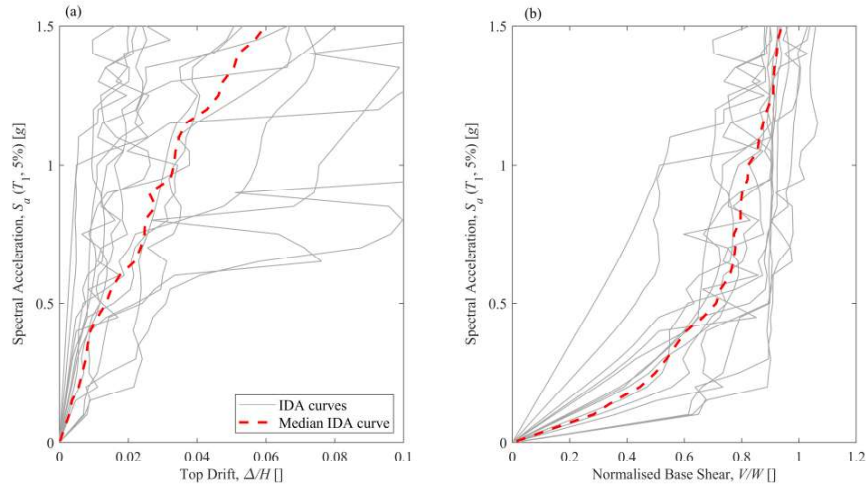


Fig. 4 – IDA curves and median IDA curves of the pier with SMA bars (a) top drift, (b) normalised base shear

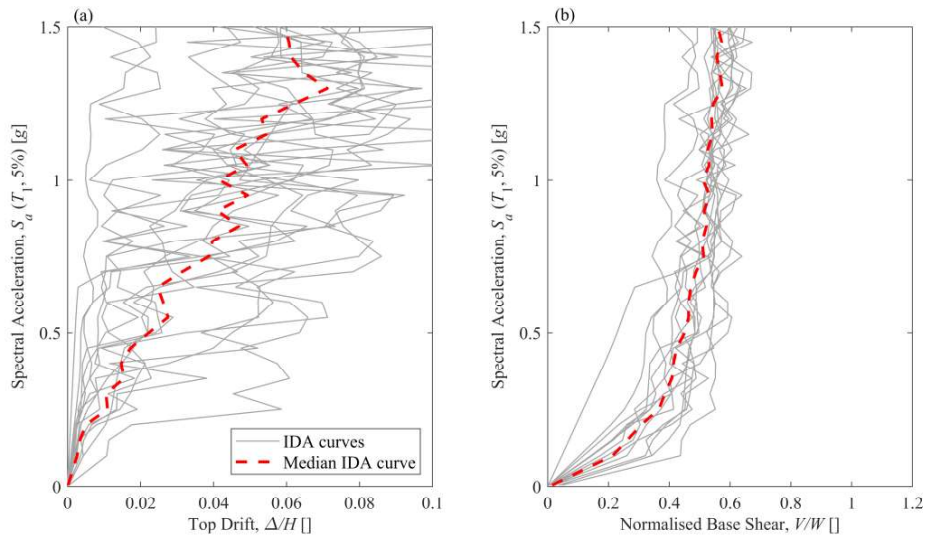


Fig. 5 – IDA curves and median IDA curves of the pier with no SMA bars (a) top drift, (b) normalised base shear

#### 4. Conclusions

This paper presents nonlinear cyclic behaviour of SMA-equipped PPS piers. In order to model piers, an experimentally validated FE model is used and a parametric study is performed to investigate the energy dissipation capacity of the SMA-equipped piers. It is found from the results of nonlinear cyclic analysis that there is both optimum length and area for the SMA bars, which leads to the highest energy dissipation ratio. Results show that well designed SMA-equipped piers can provide high energy dissipation capacity. Furthermore, IDA results showed that SMA bars can sufficiently reduce the drift response of the piers.

## References

- Shim CS, Chung C-H, Kim HH. Experimental evaluation of seismic performance of precast segmental bridge piers with a circular solid section. *Engineering Structures* 2008;30. <https://doi.org/10.1016/j.engstruct.2008.07.005>.
- Dawood H, Elgawady M, Hewes J. Behavior of segmental precast posttensioned bridge piers under lateral loads. *Journal of Bridge Engineering* 2012. [https://doi.org/10.1061/\(ASCE\)BE.1943-5592.0000252](https://doi.org/10.1061/(ASCE)BE.1943-5592.0000252).
- Tazarv M, Saiid Saiidi M. Low-Damage Precast Columns for Accelerated Bridge Construction in High Seismic Zones. *Journal of Bridge Engineering* 2016;21. [https://doi.org/10.1061/\(ASCE\)BE.1943-5592.0000806](https://doi.org/10.1061/(ASCE)BE.1943-5592.0000806).
- Z.B. Haber. Precast Column-Footing Connections for Accelerated Bridge Construction in Seismic Zones, ProQuest Dissertations and Theses. 2013.
- Song G, Ma N, Li H-N. Applications of shape memory alloys in civil structures. *Engineering Structures* 2006;28:1266–74. <https://doi.org/10.1016/j.engstruct.2005.12.010>.
- M Saiid Saiidi; Wang H. Exploratory Study of Seismic Response of Concrete Columns with Shape Memory Alloys Reinforcement. *ACI Structural Journal* 2006;103:436–43.
- DesRoches R, McCormick J, Delemont M. Cyclic Properties of Superelastic Shape Memory Alloy Wires and Bars. *Journal of Structural Engineering* 2004;130:38–46. [https://doi.org/10.1061/\(ASCE\)0733-9445\(2004\)130:1\(38\)](https://doi.org/10.1061/(ASCE)0733-9445(2004)130:1(38)).
- McKenna F. OpenSees: A framework for earthquake engineering simulation. *Computing in Science and Engineering* 2011. <https://doi.org/10.1109/MCSE.2011.66>.
- Ahmadi E, Kashani MM. Numerical investigation of nonlinear static and dynamic behaviour of self-centring rocking segmental bridge piers. *Soil Dynamics and Earthquake Engineering* 2020;128:105876. <https://doi.org/10.1016/j.soildyn.2019.105876>.
- Li C, Hao H, Bi K. Numerical study on the seismic performance of precast segmental concrete columns under cyclic loading. *Engineering Structures* 2017;148. <https://doi.org/10.1016/j.engstruct.2017.06.062>.
- Pacific Earthquake Engineering Research Center. PEER Ground Motion Database. Shallow Crustal Earthquakes in Active Tectonic Regimes, NGA-West2 2017 n.d.